

Multi-Source Uncertain Information Fusion Method for Fault Diagnosis Based on Evidence Theory

Jinhua Mi*

School of Automation Engineering
University of Electronic Science and Technology of China
Chengdu, China
jinhuaami@uestc.edu.cn

Yuhua Cheng*

School of Automation Engineering
University of Electronic Science and Technology of China
Chengdu, China
yhcheng@uestc.edu.cn

Xinyuan Wang

School of Automation Engineering
University of Electronic Science and Technology of China
Chengdu, China
wangxinyuan96@outlook.com

Songyi Zhang

School of Automation Engineering
University of Electronic Science and Technology of China
Chengdu, China
zhangsongyi@outlook.com

Abstract—Because of the measurement error and impact of other external factors, the experimentally measured fault information of rotary machinery equipment is with randomness and uncertainty. The diagnosis result gotten with uncertain information will not be accurate. Multi-source information fusion and fault identification based on cloud model and D-S evidence theory is studied in this paper. The rough set theory is used to screen and reduce the multiple fault attribute, then get the fewest fault features which also satisfy the diagnosis. The multi-source information are fused by the calculation of cloud parameters and evidence theory. At last, two kinds of rolling bearing fault databases from experiments are performed, and the diagnosis results have proved the validity and feasibility of the proposed method.

Keywords—multi-source information fusion; rotary machinery equipment; D-S evidence theory; cloud model, fault diagnosis.

I. INTRODUCTION

Through long-term production practice, it has been found that pattern recognition and fault diagnosis only based on the information collected by a single sensor will inevitably be affected by complex and changeable external factors in the actual use process. In engineering practice, it is necessary to combine various information obtained through multiple channels in different ways to make better decisions. However, information usually contains a variety of uncertainties, ambiguity and inaccuracy. The information fusion method [1], which can process the information that jointly gotten by multiple sensors, is not only theoretically feasible but also of considerable significance to fault diagnosis.

Dempster-Shafer (D-S) evidence theory [5], established by Dempster and Shafer in the late 1960s and early 1970s, is a data fusion theory widely used to process complementary information and uncertain information. The cloud model [9] is an uncertainty model that can be used to convert between qualitative concepts and quantitative values based on traditional probability and statistics theory and fuzzy theory. It can express data more accurate as a concept to discover

authentic and complete knowledge. The following section II will give a brief introduction to some of the conceptual and numerical features of the cloud model. Because of the uncertainty of the final fusion caused by the measurement errors of different types of sensors and various information sources in multi-source information, the method with a combination of cloud model and D-S evidence theory is introduced to study the multi-source information fusion in fault diagnosis for rotary machinery equipment.

II. MULTI-SOURCE INFORMATION FUSION AND PATTERN RECOGNITION METHOD BASED ON CLOUD MODEL AND D-S EVIDENCE THEORY

For the particularity of multi-source and heterogeneous information fusion, decision-making level fusion is carried out at the highest level of information representation. The information obtained by each sensor is processed separately, that is, fault information acquisition, feature extraction and fault diagnosis recognition are conducted respectively, and preliminary judgment and conclusion on the same fault are established. The fusion center then takes a vote to obtain the final identification conclusion. The specific process is shown in the Fig.1.

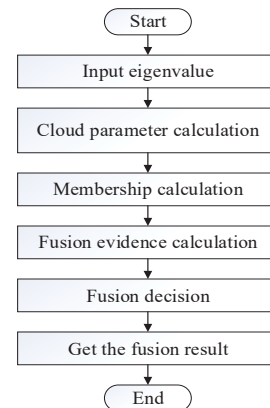


Figure. 1 The specific process.

A. Calculation of Cloud Model Parameters

Assume there are n kinds of faults in the fault knowledge base: F_1, F_2, \dots, F_n , and there are k characteristic parameters for each type of fault: $F_i = (x_{i1}, x_{i2}, \dots, x_{ik})$. For the i -th fault F_i in the fault knowledge base, select the m -group data in one experiment and construct the fault knowledge base through the eigenvalues processed by the time-frequency feature. That is, there are a total of m values for x_{ij} in F_i , then it is recorded as $x_{ij}^* = (x_{ij1}, x_{ij2}, \dots, x_{ijm})$, each feature parameter can be represented by a cloud parameter. The mathematical expectation [13] and standard deviation to build a cloud model of the fault pattern library can be calculated directly:

$$\begin{aligned} E_{xij} &= \bar{x}_{ij} = \sum_{z=1}^m x_{ijz} / m \\ E_{nij} &= \sigma_{xij} = \sqrt{\frac{1}{m} \sum_{z=1}^m (x_{ijz} - \bar{x}_{ij})^2} \\ H_{eij} &= \lambda \end{aligned} \quad (1)$$

where E_{xij} , E_{nij} and H_{eij} are the expectation, entropy and super entropy of the cloud model of the j -th parameter of the i -th fault in the fault pattern library obtained from the experimental data. And λ is a constant determined based on the ambiguity and randomness of the specific parameters.

B. Membership Calculation

For the fault signal obtained in the fault identification, assume that the fault signal is subjected to time-frequency analysis to obtain k characteristic parameters, namely $t = (t_1, t_2, \dots, t_k)$, where $t_j, j = (1, 2, \dots, k)$ is the j -th characteristic parameter of the fault signal. Then, the membership degree of the fault signal relative to the fault mode library can be calculated according to the cloud model parameters of the fault mode library and the characteristic parameters of the fault signal in section A:

$$\mu_{ij} = \exp\left(\frac{-(t_j - E_{xij})^2}{2(E'_{nij})^2}\right) \quad (2)$$

where E_{xij} is the expected value obtained according to (1), E'_{nij} is the normal random number generated by entropy E_{nij} as the expectation and hyper entropy H_{eij} as the standard deviation.

Then we have the membership matrix [14]:

$$R_{k \times n} = \begin{pmatrix} \mu_{11} & \mu_{21} & \dots & \mu_{n1} \\ \mu_{12} & \mu_{22} & \dots & \mu_{n2} \\ \vdots & \vdots & \ddots & \vdots \\ \mu_{1k} & \mu_{2k} & \dots & \mu_{nk} \end{pmatrix} \quad (3)$$

C. Fusion Evidence Calculation

In order to improve the accuracy and credibility of the final decision, the obtained membership matrix will be processed and transformed to obtain the evidence of fusion. Firstly, normalize each row of elements of the membership matrix,

$$\gamma_{ij} = \mu_{ij} / \sum_{i=1}^n \mu_{ij}, j = 1, 2, \dots, k \quad (4)$$

If θ is used to represent uncertainty, then,

$$\theta_j = 1 - \max(\mu_{1j}, \mu_{2j}, \dots, \mu_{nj}) \quad (5)$$

Based on the above analysis, the basic probability assignment function can be obtained as:

$$\begin{cases} m(U_j) = \theta_j, j = 1, 2, \dots, k \\ m(R_{ij}) = (1 - \theta_j) \gamma_{ij}, i = 1, 2, \dots, n \end{cases} \quad (6)$$

where $m(U_j)$ represents the basic probability assignment of the uncertainty of the j -th evidence, and $m(R_{ij})$ represents the basic probability assignment of the j -th characteristic parameter of the experimentally measured fault signal corresponding to the i -th fault in the fault pattern library. From Eqs. (3-6), we can get a basic probability assignment matrix $M_{k \times (n+1)}$ of k rows and $n+1$ column:

$$M_{k \times (n+1)} = \begin{pmatrix} m(R_{11}) & \dots & m(R_{n1}) & \theta_1 \\ m(R_{12}) & \dots & m(R_{n2}) & \theta_2 \\ \vdots & \vdots & \vdots & \vdots \\ m(R_{1k}) & \dots & m(R_{nk}) & \theta_k \end{pmatrix} \quad (7)$$

D. Fusion Decision

To improve the accuracy of fault identification, the following aspects should be considered in the decision of evidence fusion: 1) the effect of the evidence obtained from some fault insensitive characteristic parameters on the fusion results, 2) the processing of high conflict evidence, and 3) the uncertainty of fusion evidence. Take the above factors into consideration, by using the average evidence synthesis method, a new weight of fusion evidence can be obtained from the coefficient of evidence uncertainty and the coefficient of overall support. The *Dempster-Shafer's* rule is used for evidence fusion after reducing the degree of the evidence conflicts.

The fusion evidence is obtained from the eigenvalues of the fault signal, and each piece of evidence corresponds to an eigenvalue of the fault signal. Thus, the determination of the weight coefficient is mainly considered from two aspects: a sensor measurement error and some eigenvalues that are insensitive to fault characteristics. When the uncertainty of the evidence is indicated as ω^σ , and the overall support of each piece of evidence relative to the entire piece of evidence is ω^s , then the following formula can get the final fusion of evidence,

$$\omega_j = \alpha\omega_j^\sigma + \beta\omega_j^s, j=1,2,\dots,k, 0 \leq \omega_j \leq 1, \alpha + \beta = 1 \quad (8)$$

where α, β respectively represent the proportion of the two weight coefficients in the final weight of the fusion evidence, which can be adjusted according to the specific situation, usually taking $\alpha = \beta = 1/2$.

1) The evidence uncertainty coefficient ω^σ

Assume the relative measurement error of the sensor is

$$\chi_j = \sqrt{\sigma_j^2} / E(x_j), j=1,2,\dots,k \quad (9)$$

where $E(x_j)$ and σ_j^2 represent the mean and variance of the j -th feature parameter in the fault mode library, respectively. Uncertainty of the evidence will become larger as χ_j and θ_j increase. Assume that

$$\lambda_j = 1 / (\chi_j + \theta_j), j=1,2,\dots,k \quad (10)$$

Because the weight of the corresponding j -th evidence in the fusion will decrease with the decrease of parameter λ_j .

Thus, the uncertainty coefficient ω^σ is determined by λ_j :

$$\omega^\sigma = \lambda_j / \sum_{m=1}^k \lambda_m, j=1,2,\dots,k \quad (11)$$

2) The overall support of evidence ω^s

The degree of support between evidence is determined by the distance of evidence. It is advisable to set two evidences m_j, m_h , and define the distance function [16] as follows

$$d(m_j, m_h) = \frac{\|m_j - m_h\|}{\sqrt{n}} = \sqrt{\frac{1}{n} \sum_{i=1}^n (m_{ji} - m_{hi})^2} \quad (12)$$

$j, h = 1, 2, \dots, k$

The larger the $d(m_j, m_h)$ is, the smaller the similarity between the evidences is, the similarity between the evidences is defined as

$$\xi(m_j, m_h) = 1 - d(m_j, m_h) \quad j, h = 1, 2, \dots, k \quad (13)$$

Thus, the overall support of evidence can be determined by the sum of the similarities between the evidence and other evidences:

$$\eta(m_j) = \sum_{h=1, h \neq j}^k \xi(m_j, m_h) \quad j = 1, 2, \dots, k \quad (14)$$

where $\eta(m_j)$ represents the overall support of the j -th evidence in the total evidence. A large $\eta(m_j)$, which means higher credibility of the j -th evidence in the total evidence, will lead to a greater evidence weight in the final decision, and the overall support coefficient will be

$$\omega_j^s = \eta(m_j) / \sum_{j=1}^k \eta(m_j), j = 1, 2, \dots, k \quad (15)$$

Based on the above analysis, the basic probability assignment matrix and the final weight coefficient for each

piece of evidence fusion have been obtained. To improve the efficiency and credibility of the fusion, the data from the same sensor or the same information source can be iterated. After the synthesis is averaged, the iterative evidence is finally fused by the *Dempster-Shafer's* rule of combination [17] to obtain the recognition result.

Suppose a sensor or an information source has j -values generated by eigenvalues, then the average evidence synthesis formula is as follows:

$$\begin{cases} m(U) = \sum_{j=1}^k \omega_j \cdot \theta_j \\ m(R) = \sum_{j=1}^k \omega_j \cdot m(R_{ij}), i = 1, 2, \dots, n \end{cases} \quad (16)$$

III. EXPERIMENTAL RESULTS

In this paper, from the perspective of theory to practice, the algorithm is firstly verified by the bearing data of Case Western Reserve University, and then the rolling bearing experimental platform is built to verify the feasibility of the algorithm through the experimental data. Experiments based on different data sets are described below

A. Example 1: The Data of the Case Western Reserve University

The data of rolling bearing from CWRU is chosen to validate the efficiency of the proposed method. The experimental platform details and the geometric dimensions of the bearing can be checked in [18].

1) Fault signals analysis and processing

According to time-frequency analysis method [19], features of the rolling bearing fault signal are extracted and we use ROSETTA software [20] to reduce the features, then the result is listed in TABLE I.

TABLE I. FEATURE PARAMETERS OF CWRU

Sensor	DE	FE	BA
Features	MAX, RMS, MSA, WF, PF, PEAK, CGF, FV, E2, E3, E4, E5, E6	RMS, PEAK, PF, MC, skewness, E1, E3, E6	RMS, MSA, PEAK, skewness, CGF, E1, E2, E3, E4, E7, E8

2) Multi-source uncertain information fusion and fault diagnosis experiments

In the 100 data sets with 32 feature parameters of each fault state, the first 80 data sets of each fault state are selected for cloud modeling. The rest 20 data sets are used for diagnostic testing. The specific process is as follows:

(1) Cloud model Parameter Calculation

The first 80 data sets of each fault state for rolling bearings with 32 feature parameters, which was selected by rough set theory, are set as the prior information to calculate the cloud model parameters. Let super entropy H_e equals 0.02.

The cloud parameters are computed by using MATLAB and listed in the following TABLE II and III (due to the space limit, only a fraction of the cloud parameters corresponding to some eigenvalues are listed).

TABLE II. CLOUD PARAMETER EX FOR SOME EIGENVALUES

Fault type	Feature 1	Feature 2	Feature 3	Feature 4
1	0.475949	0.139147	0.094087	1.253151
2	0.413403	0.118255	0.079254	1.260442
3	1.380173	0.291788	0.167005	1.395476
4	2.576856	0.450318	0.236245	1.480789
5	2.902777	0.772177	0.469787	1.342484
6	3.041141	0.309671	0.100727	2.102901

TABLE III. CLOUD PARAMETER EN FOR SOME EIGENVALUES

Fault type	Feature 1	Feature 2	Feature 3	Feature 4
1	0.048724	0.003251	0.002663	0.009138
2	0.039988	0.002759	0.001768	0.011045
3	0.146252	0.008384	0.004951	0.016255
4	0.255938	0.017953	0.007932	0.027809
5	0.120379	0.018624	0.014316	0.014004
6	0.404882	0.026343	0.004759	0.099622

(2) Membership Calculation

Based on the calculated cloud parameters, the membership degree of each parameter relative to the corresponding parameters of each fault state for rolling bearing can be computed by (2) and (3). The matrix is obtained in TABLE IV (due to the limitation of space, only the membership degree obtained from a test data set with slight wear of rolling body is listed here):

TABLE IV. MEMBERSHIP MATRIX

Feature	Type 1	Type 2	Type 3	Type 4	Type 5
1	0.56402	0.43598	0.00000	0.00000	0.00000
2	0.47972	0.52028	0.00000	0.00000	0.00000
3	0.41479	0.26776	0.00000	0.00000	0.00000
4	0.00639	0.99361	0.00000	0.00000	0.00000

(3) Fusion Evidence Calculation

Calculate the weight of evidence fusion, and re-allocate the basic probability assignment matrix after the fusion weights.

(4) Decision Fusion

After average iteration, three pieces of evidence for final fusion from the three end sensors of the fan end, the drive end and the base end are obtained, and merged with the Dempster-Shafer's rule of combination. As shown in the TABLE V.

TABLE V. FINAL FUSION EVIDENCE

Evidence	m1	m2	m3	Final
Type 1	0.0736	0.062082	0.11064	0.469662
Type 2	0.071518	0.057982	0.089563	0.345034
Type 3	0.044714	0.013343	0.080937	0.044861
Type 4	0.043541	0.007147	0.030134	0.008712
Type 5	0.035281	0.024758	0.045477	0.036905
Type 6	0.045484	0.034531	0.060686	0.088548
Uncertainty	0.029262	0.032132	0.007189	0.006279

From TABLE V, it can be concluded that the probability of this fault test information being the first fault type is the highest, and its probability is 0.469662. Therefore, it is judged to be a fault with the slight wear of the rolling body.

Fig.2 shows the final diagnosis based on the genetic algorithm optimization support vector machine method (SVM) [21]. And the results of the optimization evidence theory are shown in the Fig.3.

It can be seen from the final test results based on the cloud model and D-S evidence theory has the higher accuracy than the method of SVM, indicating that the multi-source information fusion and fault identification methods based on the cloud model and D-S evidence theory are effective.

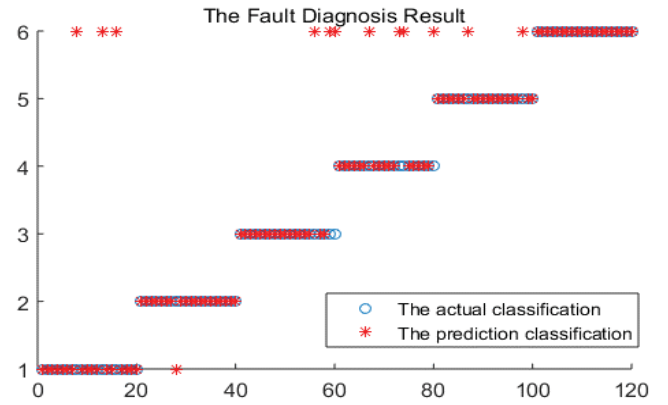


Figure 2. Test result of CWRU database based on the SVM

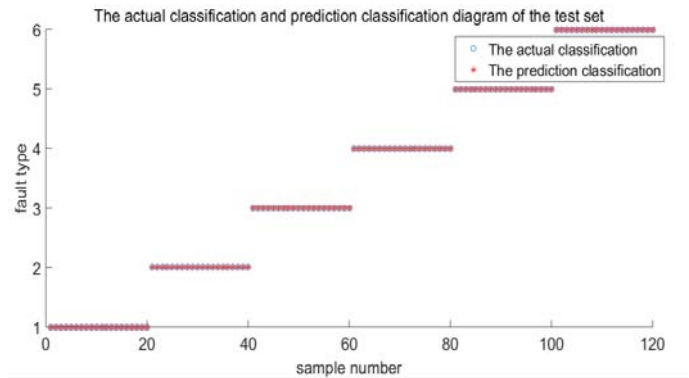


Figure 3. Test result of CWRU database based on the cloud model and D-S evidence theory

B.Example 2: The Fault Diagnosis of Rolling Bearings Based on Practical Experiment

1) Platform introduction

An experimental platform is established as shown in Fig. 4 to collect the fault data of rolling bear. Five types of fault modes for rolling bearings with fault depth of 0. 3mm are selected: (1) the slight wear of the inner ring (I1: fault circumferential dimension is 12.9°); (2) the moderate wear of the inner ring (I2: fault circumferential dimension is 38.6°); (3) the severe wear of the inner ring (I3: fault circumferential dimension is 64.3°); (4) the moderate wear of the outer ring (O2: fault circumferential dimension is 38.6° and fault

circumferential angle position is 270°); (5) the slight wear of the outer ring (O1: fault circumferential dimension is 1° and fault circumferential angle position is 270°). Two acceleration sensors (HD-YD-221) are respectively located in the vertical (a0) and horizontal (a1) directions of the bearing housing for collecting acceleration vibration signals. Three displacement sensors (v0-v2) with 8V/mm sensitivity (WT0180) are used to measure voltage information in the vertical and horizontal directions of the shaft. The sampling frequency is set as 10 kHz.

2) Analysis and Processing of Fault Signals

Time-frequency characteristic parameters are obtained for the signal collected by each sensor. We reduced the time-frequency feature parameters by ROSETTA software, which are listed in TABLE VI.

Each type of fault randomly selects 200 data sets collected by the experimental platform, and each data set is calculated from time-frequency characteristic parameters with 1024 sample points. The former 180 data sets for each fault type constitute the training set, and the later 20 data sets constitute the test set. Based on the method in Section II, the obtained cloud parameters are shown in the TABLE VII and VIII (Due to limited space, only cloud parameter calculation results of partial characteristic parameters are displayed).

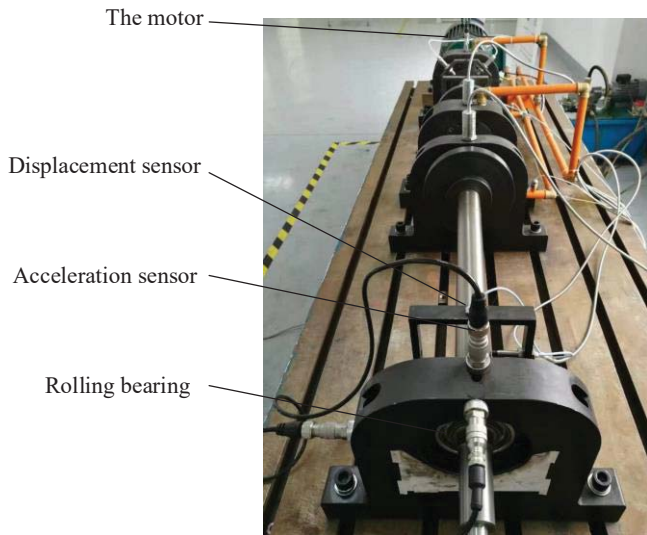


Figure. 4. The experimental platform diagram.

TABLE VI. THE FEATURES OF EXPERIMENTAL DATABASE

Sensor	Features
a0	MAX, RMS, PEAK, AA, Kurtosis, PF, MC, skewness, KF, MSF, CGF, E1, E2, E3, E4, E5, E7, E8
a1	Kurtosis, WF, PEAK, PF, MC, KF, CGF, E1, E4, E5, E7, E8
v0	RMS, MSA, AA, Kurtosis, WF, PEAK, PF, skewness, KF, CGF, FV
v1	MSA, AA, Kurtosis, WF, PEAK, PF, MC, skewness, KF, CGF, FV
v2	RMS, MSA, AA, WF, PEAK, PF, MC, skewness, MSF, CGF, E2, E3, E4, E5, E6, E7, E8

TABLE VII. CLOUD PARAMETER EX FOR PARTIAL EIGENVALUES

Fault type	Feature 1	Feature 2	Feature 3	Feature 4	Feature 5
1	1.176944	0.140942	0.068728	23.04403	8.364193
2	0.873313	0.086087	0.048262	28.03696	10.05397
3	1.860056	0.148532	0.069856	53.84926	12.42827
4	1.159976	0.138253	0.07135	21.30163	8.383923
5	0.242099	0.033031	0.022549	12.78776	7.31689

TABLE VIII. CLOUD PARAMETER EN FOR PARTIAL EIGENVALUES

Fault type	Feature 1	Feature 2	Feature 3	Feature 4	Feature 5
1	0.146422	0.010377	0.003654	3.623971	1.007396
2	0.245993	0.007345	0.002198	13.30288	2.299932
3	0.487429	0.016437	0.003869	22.3623	2.368586
4	0.200081	0.009897	0.003603	3.907296	1.25637
5	0.039603	0.00185	0.000744	3.030675	1.052872

70 characteristic parameters of 20 sets of test data for each fault type are gotten, and then calculate the membership degree of the test data through the cloud parameters of the fault knowledge base. The membership matrix is processed and transformed. Through the average iteration, five pieces of evidence from five different sensors are obtained. After the Dempster-Shafer's rule of combination, the final fusion results are shown in TABLE IX (take the slight wear of the inner ring as an example).

The final diagnosis and analysis of test set data based on the SVM and the cloud model optimized D-S evidence theory are as Fig. 5 and Fig.6. It can be seen that the accuracy of SVM is 84% while the final 20 test data can be correctly diagnosed and identified by the cloud model optimized D-S evidence theory, and the accuracy rate is 100%.

TABLE IX. FINAL FUSION EVIDENCE

Evidence	Type 1	Type 2	Type 3	Type 4	Type 5	Un-certainty
m1	0.0338	0.0300	0.0320	0.0310	0.0162	0.0024
m2	0.0233	0.0179	0.0291	0.008	0.0052	0.0085
m3	0.0276	0.0046	0.0116	0.0247	0.0089	0.0022
m4	0.0512	0.0057	0.0027	0.0029	0.0043	0.0046
m5	0.1298	0.1199	0.1225	0.1227	0.1124	0.0046
Final	0.949	0.0112	0.0237	0.0133	0.0024	0.00001

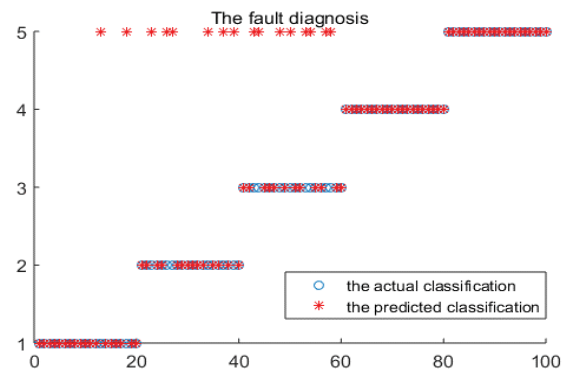


Figure 5. The diagnosis results of SVM method.

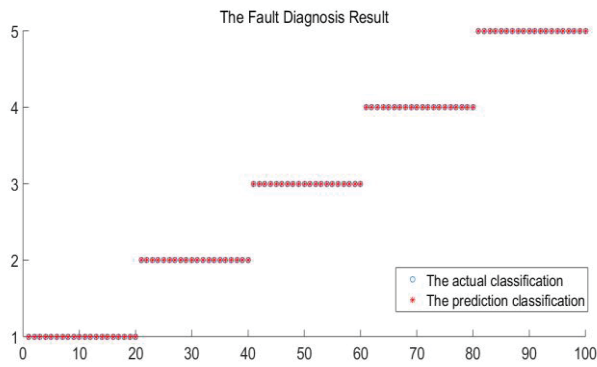


Figure. 6 The final diagnosis based on the cloud model and D-S evidence theory.

IV. CONCLUSIONS

Due to the measurement error of the sensor and the randomness of the rolling bearing fault, the rolling bearing fault information measured by the experiment has the characteristics of randomness and uncertainty. In this paper, a rolling bearing fault diagnosis system is constructed based on multi-source uncertain information fusion method. This paper studies the multi-source information fusion and fault identification method based on cloud model and D-S evidence theory. The main research work of this paper is summarized as follows:

Firstly, for the fusion of multi-source information, rough set theory is used to screen fault characteristic parameters. Then, according to the cloud model and the basic operation of D-S evidence theory, cloud parameters are calculated and evidence bodies are processed. Finally, the method of evidence theory is adopted to fuse multi-source information. Experimental results show that the technique of multi-source information fusion and fault identification based on cloud model and D-S evidence theory is effective in fault diagnosis of rolling bearing.

ACKNOWLEDGMENT

This work was partially supported by the National Natural Science Foundation of China under contract No. 51805073 and U1830207, the Chinese Universities Scientific Fund under contract No.ZYGX2018J061, and the Sichuan Science and Technology Project under contract No. 2019JDJQ0015. The authors wish to acknowledge the technical support of Wuxi Houde Automation Meter Co., LTD.

REFERENCES

[1] X. Che, J. Mi, D. Chen. "Information fusion and numerical characterization of a multi-source information system." *Knowledge-Based Systems*, vol.145, pp. 121-133, 2018.

[2] H. Cheng, J. Zhao, M. Fu. "Research on the method of multi-source information fusion based on Bayesian theory." 2018 IEEE 3rd Advanced Information Technology, Electronic and Automation Control Conference (IAEAC). IEEE, 2018.

[3] G. Liu, J. Liu, R. Wei, J. Wang. "Multi-source data fusion technology for power wearable system." 2018 IEEE International Conference on Computer and Communication Engineering Technology (CCET). IEEE, pp. 118-122, 2018.

[4] W. Wei, J. Liang. "Information fusion in rough set theory: An overview." *Information Fusion*, vol. 48, pp. 107-118, 2019.

[5] B. C. Chen, X. Tao, M. R. Yang, C. Yu, W.M. Pan, V.C. Leung. "A saliency map fusion method based on weighted DS evidence theory." *IEEE Access*, vol. 6, pp. 27346-27355, 2018.

[6] H. Lei, Z. Yang, Z. Zhang, W. Wang. "Multi-image source target fusion detection based on DS evidence theory." *Journal of Physics: Conference Series*, vol. 1168, no. 4. IOP Publishing, 2019.

[7] Y. Lin, Y. Li, X.Yin, Z. Dou. "Multisensor fault diagnosis modeling based on the evidence theory." *IEEE Transactions on Reliability*, vol. 67, no. 2, pp. 513-521, 2018.

[8] E. Lefevre, O. Colot, P. Vannooenbergh. "Belief function combination and conflict management." *Information Fusion*, vol. 3, no. 2, pp.149-162, 2002.

[9] H.G.Peng, J.Q. Wang. "A Multicriteria Group Decision-Making Method Based on the Normal Cloud Model With Zadeh's Z-Numbers." *IEEE Transactions on Fuzzy Systems* 26.6 (2018): 3246-3260.

[10] D. Y. Li, C. Y. Liu, W. Y. Gan. "A new cognitive model: cloud model." *International Journal of Intelligent Systems*, vol. 24, pp. 357-375, 2009.

[11] G. Y. Wang, C. L. Xu, D. Y. Li. "Generic normal cloud model." *Information Sciences*, vol. 280, pp. 1-15, 2014.

[12] H. C. Liu, L. E. Wang, Z. Li, Y. P. Hu. "Improving risk evaluation in FMEA with cloud model and hierarchical TOPSIS method." *IEEE Transactions on Fuzzy Systems* vol. 27, no.1, pp. 84-95, 2019.

[13] C. S. Feng. Rolling bearing diagnosis research of CNC machine tools based on multi source information fusion. Qingdao Technological University, 2015.

[14] H. J. Liu, Z. Liu, W. Jiang, Y. Y. Zhou. "A Method for Emitter Recognition Based on Cloud Model." *Journal of Electronics & Information Technology*, vol. 31, no. 9, 2009.

[15] C. S. Shieh, C. T. Lin. "A vector neural network for emitter identification." *IEEE Transactions on Antennas and Propagation*, vol. 50, no. 8, pp. 1120-1127, 2002.

[16] X. Z. Yin, J. G. Wang. "A solution to the problem of evidence conflict in heterogeneous source information fusion." *Journal of Astronautics*, vol.30, no. 4, 2009.

[17] Smets P, Analtzing the combining of conflicting belief functions[J].*Information Fusion*, 2007,8(4):387-412.

[18] K. A. Loparo, Bearings vibration data set. Case Western Reserve University.

[19] X. M. Xue, J. Z. Zhou, "A hybrid fault diagnosis approach based on mixed-domain state features for rotating machinery." *ISA transactions*, vol. 66, pp. 284-295, 2017.

[20] L. X. Shen, F. E. H. Tay, L. S. Qu, Y. D. Shen, "Fault diagnosis using rough sets theory." *Computers in industry*, vol.43, no. 1, pp. 61-72, 2000.

[21] V. N. Vapnik, *The Nature of Statistical Learning Theory*. 1st ed. New York: Spring – Verlag, 1995.